



Computational studies of 1,2-disubstituted benzimidazole derivatives

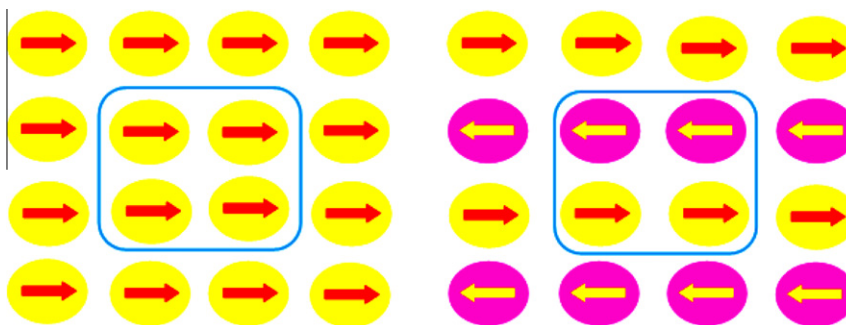
J. Jayabharathi*, V. Thanikachalam, K. Jayamoorthy, M. Venkatesh Perumal

Department of Chemistry, Annamalai University, Annamalinagar 608 002, India

HIGHLIGHTS

- Steric interaction must be reduced in order to obtain larger β_0 values.
- NBO analysis elucidates the delocalization within the molecule.
- Probable charge transfer (CD) taking place inside the chromophore.
- Charge distribution was calculated by NBO and Mulliken methods.

GRAPHICAL ABSTRACT



ARTICLE INFO

Article history:

Received 8 May 2012

Received in revised form 18 May 2012

Accepted 29 May 2012

Available online 6 June 2012

Keywords:

AIM
DFT
NLO
NBO
XRD
MEP

ABSTRACT

Some 1,2-disubstituted benzimidazole derivatives (**1–6**) have been synthesized and characterized by mass, ^1H , ^{13}C NMR and elemental analysis. XRD analysis was carried out for 1-(4-methylbenzyl)-2-*p*-tolyl-1H-benzo[d]imidazole. Calculated bond lengths, bond angles and thus dihedral angles are found to be slightly higher than that of X-ray diffraction values of its experimental data. The charge distribution has been calculated from the atomic charges by non-linear optical (NLO) and natural bond orbital (NBO) analyses have been calculated by ab initio method. Since the synthesized 1,2-disubstituted benzimidazole derivatives have the largest μ_g/β_0 value and can be used as potential NLO materials. Analysis of the molecular electrostatic potential (MEP) energy surface exploited the region for non-covalent interactions in the molecule. Atom in molecule analysis (AIM) was carried out to show the presence of bond critical points (BCPs).

© 2012 Elsevier B.V. All rights reserved.

Introduction

Benzimidazole based chromophores have received increasing attention due to their distinctive linear, non-linear optical properties and also due to their excellent thermal stability in guest–host systems [1]. The imidazole ring can be easily tailored to accommodate functional groups, which allows the covalent incorporation of the NLO chromophores into polyamides leading to NLO side chain polymers [2]. Most π -conjugated systems play a major role in determining second-order NLO response [3]. Searching organic materials with non-linear optical (NLO) properties is usually con-

centrated on molecules with donor–acceptor π -conjugation (D- π -A) and deals with the substituent effects on the degree of π -conjugation, steric hindrance and the hyperpolarizability of the substances [4]. Nowadays there is an insufficient understanding for designing optimal NLO materials, even certain classes of D- π -A compounds were theoretically studied [5]. Not only the push–pull effect in D- π -A compounds quantified, but also a linear dependence of the push–pull quotient (π^*/π) on molar hyperpolarizability were detected [6]. Thus, π^*/π is a sensitive parameter of the donor–acceptor quality of compounds for potential NLO applications.

Our approach is to design newly π -conjugated benzimidazole derivatives to use as materials in material chemistry [7,8]. Hence there is considerable interest in the synthesis of new materials with optical non-linearity by virtue of their potential use in device

* Corresponding author. Tel.: +91 9443940735.

E-mail address: jtchalam2005@yahoo.co.in (J. Jayabharathi).

applications related to telecommunications, optical computing, optical storage, and optical information processing [9–12]. Herein we report the synthesis and theoretical studies of some benzimidazole derivatives (**1–6**).

Experimental

Spectral measurements

NMR spectra were recorded on Bruker 400 MHz NMR spectrometer. Mass spectrum was recorded using Agilent 1100 Mass spectrometer.

Non-linear optical measurements

The non-linear optical conversion efficiencies were parted using a modified set up of Kurtz and Perry. A Q-switched Nd:YAG laser beam of wavelength of 1064 nm was used with an input power of 4.1 mJ/pulse width of 10 ns, scattering geometry 90°, the repetition rate being 10 Hz, monochromator Jobin Youon Triax 550, slit width 0.5 mm, focal length of focusing lens 20 cm, PMT model number XP2262B used in Philips photonics, power supply for PMT is 1.81 KU/mA with oscilloscope Jektronix TDS 3052B.

Computational details

Quantum mechanical calculations were used to carry out the optimized geometry, NLO, NBO and HOMO–LUMO analysis with Gaussian-03 program using the Becke3–Lee–Yang–Parr (B3LYP) functional supplemented with the standard 6-31G(d,p) basis set [13]. As the first step of our DFT calculation for NLO, NBO and HOMO–LUMO analysis, the geometry taken from the starting structures were optimized and then, the electric dipole moment μ and β tensor components of the studied compounds were calculated, which has been found to be more than adequate for obtaining reliable trends in the first hyperpolarizability values.

We have reported the β_{tot} (total first hyperpolarizability) for the investigated molecules and the components of the first hyperpolarizability can be calculated using equation:

$$\beta_i = \beta_{\text{iii}} + 1/3 \sum_{i \neq j} (\beta_{\text{ijj}} + \beta_{\text{jjj}} + \beta_{\text{iji}}) \quad (1)$$

Using the x , y and z components, the magnitude of the first hyperpolarizability tensor can be calculated by

$$\beta_{\text{tot}} = (\beta_x^2 + \beta_y^2 + \beta_z^2)^{1/2} \quad (2)$$

The complete equation for calculating the magnitude of first hyperpolarizability from Gaussian-03 output is given as follows:

$$\beta_{\text{tot}} = [(\beta_{\text{xxx}} + \beta_{\text{yyy}} + \beta_{\text{zzz}})^2 + (\beta_{\text{yyy}} + \beta_{\text{yzz}} + \beta_{\text{yxx}})^2 + (\beta_{\text{zzz}} + \beta_{\text{zxx}} + \beta_{\text{zyy}})^2]^{1/2} \quad (3)$$

All the electric dipole moment and the first hyperpolarizabilities are calculated by taking the Cartesian coordinate system (x , y , z) = (0, 0, 0) at own center of mass of the compounds.

Natural bond orbital (NBO) analysis

NBO analysis have been performed on the molecule at the DFT/B3LYP/6-31G(d,p) level in order to elucidate the intramolecular, rehybridization and delocalization of electron density within the molecule. The second order Fock matrix was carried out to evaluate the donor–acceptor interactions in the NBO analysis [14]. The interactions result in a loss of occupancy from the localized NBO of the idealized Lewis structure into an empty non-Lewis orbital.

For each donor (i) and acceptor (j), the stabilization energy $E(2)$ associated with the delocalization $i \rightarrow j$ is estimated as

$$E(2) = \Delta E_{ij} = q_i \frac{F(i,j)^2}{\varepsilon_j - \varepsilon_i} \quad (4)$$

where q_i is the donor orbital occupancy, ε_i and ε_j are diagonal elements and $F(i,j)$ is the off diagonal NBO Fock matrix element [15]. The larger the $E(2)$ value, the more intensive is the interaction between electron donors and electron acceptors, i.e., the more donating tendency from electron donors to electron acceptors and the greater the extent of charge transfer or conjugation of the whole system.

General procedure for the synthesis of ligands

A mixture of corresponding aldehyde (2 mmol), *o*-phenylenediamine (1 mmol) and ammonium acetate (2.5 mmol) has been refluxed at 80 °C in ethanol for appropriate time. The reaction was monitored by TLC and purified by column chromatography using petroleum ether: ethyl acetate (9:1) as the eluent.

Results and discussion

1,2-Disubstituted benzimidazole: X-ray analysis

1-(4-Methyl benzyl)-2-*p*-tolyl-1H-benzo[d]imidazole [16] is a triclinic crystal. It crystallizes in the space group $P\bar{1}$. The cell dimensions are $a = 9.6610 \text{ \AA}$, $b = 10.2900 \text{ \AA}$, $c = 17.7271 \text{ \AA}$. ORTEP diagram of **5** (Fig. 1) shows that the benzimidazole ring is essentially planar. The dihedral angles between the planes of the benzimidazole and the benzene rings of the 4-methylbenzyl and the *p*-tolyl groups are 76.64(3)° and 46.87(4)°, respectively, in molecule A. The corresponding values in molecule B are 86.31(2)° and 39.14(4)°. The dihedral angle between the planes of the two benzene rings is 73.73(3)° and 80.69(4)° in molecules A and B, respectively. Optimization of **5** have been performed by DFT at B3LYP/6-31G(d,p) using Gaussian-03. All these XRD data are in good agreement with the theoretical values (Table 1). However, from the theoretical values it can be found that most of the optimized bond lengths, bond angles and dihedral angles are slightly higher than that of XRD values. These deviations can be attributed to the fact that the theoretical calculations were aimed at the isolated molecule in the gaseous phase and the XRD results were aimed at the molecule in the solid state.

The key twist, designated as α have been examined. α is used to indicate the twist of benzimidazole ring from the aromatic six-membered ring at C-2. The twist originates from the interaction of substituent at benzyl rig attached nitrogen of the benzimidazole with the substituent at C-2. The present structural information allows us to further explore the correlation between structural features and fluorescent property. When the two adjacent aromatic species are in a coplanar geometry, the *p*-orbitals from the C–C bond connecting the two species will have maximal overlapping and the two rings will have a rigid and partial delocalized conjugation, as the result, the bond is no longer a pure single bond, as evident from the X-ray data.

Second harmonic generation (SHG) studies of 1,2-disubstituted benzimidazole derivatives

Second harmonic signals of 45 (**1**), 47 (**2**), 51 (**3**), 46 (**4**), 54 (**5**) and 52 (**6**) mV was obtained for 1,2-disubstituted benzimidazole derivatives by an input energy of 4.1 mJ/pulse. But the standard KDP crystal gave a SHG signal of 110 mV/pulse for the same input energy. The second order non-linear efficiency will vary with the particle size of the powder sample [17]. Higher efficiencies are achieved by optimizing the phase matching [18]. On a molecular

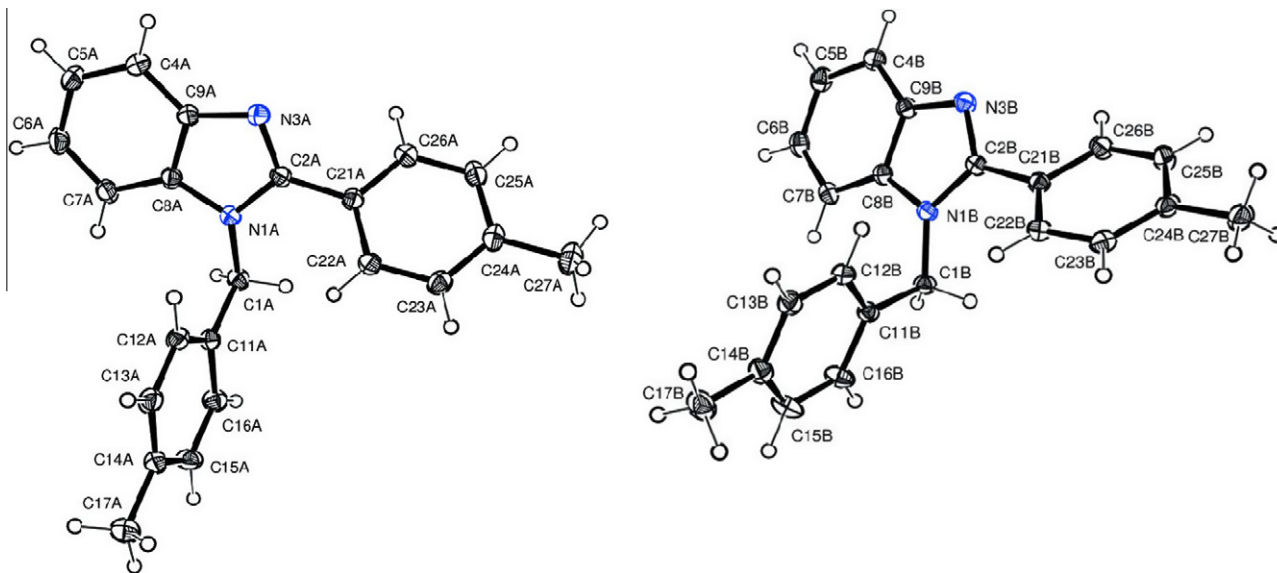


Fig. 1. ORTEP diagram of 5 with 30% probability.

Table 1
Selected bond lengths (Å), bond angles (°) and torsional angles (°) of 5.

Bond lengths (Å)	Experimental XRD (Å)	Bond angles (°)	Experimental XRD (°)	Torsional angles (°)	Experimental XRD (°)
N1A–C2A	1.3782(1.4972)	C2A–N1A–C8A	106.23(101.69)	C2A–N1A–C1A–C11A	109.45(–177.75)
N1A–C8A	1.3833(1.4584)	C2A–N1A–C1A	128.33(113.71)	C8A–N1A–C1A–C11A	–81.12(–62.25)
N1A–C1A	1.4537(1.4700)	C8A–N1A–C1A	124.79(113.33)	C9A–N3A–C2A–N1A	–0.02(–13.69)
N3A–C2A	1.3163(1.3671)	C2A–N3A–C9A	104.77(105.49)	C9A–N3A–C2A–C21A	–178.71(165.91)
N3A–C9A	1.3881(1.4606)	C2B–N1B–C8B	106.27(101.69)	C8A–N1A–C2A–N3A	0.59(17.54)
N1B–C2B	1.3795(1.4972)	C2B–N1B–C1B	129.32(113.71)	C1A–N1A–C2A–N3A	171.55(139.72)
N1B–C8B	1.3863(1.4584)	C8B–N1B–C1B	123.98(113.33)	C8A–N1A–C2A–C21A	179.28(–162.06)
N1B–C1B	1.4550(1.4700)	C2B–N3B–C9B	105.12(105.41)	C1A–N1A–C2A–C21A	–9.75(–39.88)
N3B–C2B	1.3174(1.3671)	N1A–C1A–C11A	115.07(109.47)	C9A–C4A–C5A–C6A	0.1(–0.1581)
N3B–C9B	1.3866(1.4606)	N3A–C2A–N1A	113.25(113.53)	C2A–N1A–C8A–C7A	178.45(166.15)
C1A–C11A	1.5135(1.5400)	N3A–C2A–C21A	123.44(123.23)	C1A–N1A–C8A–C7A	7.08(43.71)
C2A–C21A	1.4729(1.5400)	N1A–C2A–C21A	123.30(123.24)	C2A–N1A–C8A–C9A	–0.88(13.70)
C7A–C8A	1.3921(1.3862)	N1A–C8A–C3A	131.76(130.72)	C1A–N1A–C8A–C9A	–172.25(136.15)
C8A–C9A	1.3999(1.4763)	N1A–C8A–C9A	103.49(108.25)	C6A–C7A–C8A–N1A	179.75(176.19)
C14A–C17A	1.5089(1.5400)	N3A–C9A–C4A	129.91(130.69)	C2B–N1B–C1B–C11B	108.10(–177.75)
C24A–C27A	1.5078(1.5400)	N3A–C9A–C8A		C8B–N1B–C1B–C11B	–79.66(–62.25)
			110.26(108.25)	C9B–N3B–C2B–N1B	–0.86(–13.69)
				C9B–N3B–C2B–C21B	177.35(165.91)
				C8B–N1B–C2B–N3B	1.24(17.54)
				C1B–N1B–C2B–N3B	173.85(139.72)
				C8B–N1B–C2B–C21B	–176.90(162.06)
				C1B–N1B–C2B–C21B	–4.29(–39.88)
				C9B–C4B–C5B–C6B	0.25(–0.1581)
				C2B–N1B–C8B–C7B	176.39(166.15)
				C1B–N1B–C8B–C7B	3.28(43.71)
				C2B–N1B–C8B–C9B	–1.05(–13.70)
				C1B–N1B–C8B–C9B	–174.15(–136.15)
				C6B–C7B–C8B–N1B	177.76(176.19)

Values within the parenthesis corresponds to theoretical values.

scale, the extent of charge transfer (CT) across the NLO chromophore determines the level of SHG output, the greater the CT and the larger the SHG output.

Comparison of $\mu\beta_0$

The overall polarity of the synthesized 1,2-disubstituted benzimidazole derivatives was small when their dipole moment aligned in a parallel fashion (Fig. 2). When the electric field is removed, the parallel alignment of the molecular dipole moments begins to deteriorate and eventually the imidazole derivative loses its NLO

activity. The ultimate goal in the design of polar materials is to prepare compounds which have their molecular dipole moments aligned in the same direction [19].

Theoretical investigation plays an important role in understanding the structure–property relationship, which is able to assist in designing novel NLO chromophores. The electrostatic first hyperpolarizability (β) and dipole moment (μ) of the imidazole chromophore have been calculated by using Gaussian 03 package [20]. From Table 2, it is found that the 1,2-disubstituted benzimidazole derivatives show larger $\mu\beta_0$ values, which is attributed to the positive contribution of their conjugation.

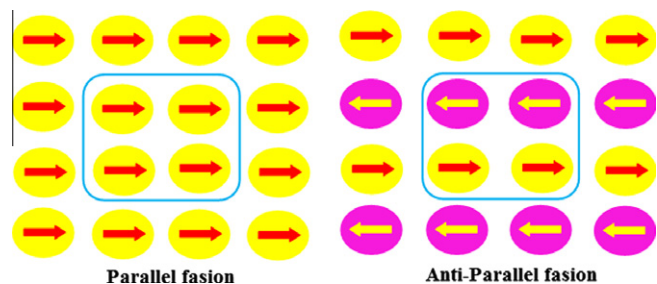


Fig. 2. Orientation of dipole moments.

Octupolar and dipolar components of 1,2-disubstituted benzimidazole derivatives

The 1,2-disubstituted benzimidazole derivatives possess a more appropriate ratio of off-diagonal versus diagonal β tensorial component ($r = \beta_{xyy}/\beta_{xxx}$) which reflects the inplane non-linearity anisotropy and the largest $\mu\beta_0$ values. The difference of the β_{xyy}/β_{xxx} ratios can be well understood by analyzing their relative molecular orbital properties. The r values of 1,2-disubstituted benzimidazole derivatives are 0.0579 (1), -0.0125 (2), -0.2037 (3), 0.0772 (4), -0.0800 (5), -0.2275 (6). The electrostatic first hyperpolarizabilities (β_0) and dipole moment (μ) of the chromophores have been investigated theoretically. These observed results can be explained by the reduced planarity in such chromophores caused by the steric interaction azomethine nitrogen atom. Hence, the steric interaction must be reduced in order to obtain larger β_0 values.

The β tensor [21] can be decomposed in a sum of dipolar ($\sum_{j=1}^{2D} \beta$) and octupolar ($\sum_{j=3}^{2D} \beta$) tensorial components, and the ratio of these two components strongly depends on their 'r' ratios. Complying with the Pythagorean theory and the projection closure condition, the octupolar and dipolar components of the β tensor can be described as:

$$\|\sum_{j=1}^{2D} \beta\| = (3/4)[(\beta_{xxx} + \beta_{xyy})^2 + [(\beta_{yyy} + \beta_{yxx})^2]] \tag{5}$$

$$\|\sum_{j=1}^{2D} \beta\| = (1/4)[(\beta_{xxx} - 3\beta_{xyy})^2 + [(\beta_{yyy} + \beta_{yxx})^2]] \tag{6}$$

The parameter $\rho^{2D} [\rho^{2D} = \|\sum_{j=1}^{2D} \beta\|]$ is convenient to compare the relative magnitudes of the octupolar and dipolar components of β . The observed positive small ρ^{2D} value reveals that the β_{iii}

component cannot be zero and these are dipolar component. Since most of the practical applications for second order NLO chromophores are based on their dipolar components, this strategy is more appropriate for designing highly efficient NLO chromophores.

Natural bond orbital (NBO) analysis

NBO analysis have been performed for 1,2-disubstituted benzimidazole derivatives at the DFT/B3LYP/6-31++G(d,p) level in order to elucidate the intramolecular, hybridization and delocalization of electron density within the molecule. The importance of hyperconjugative interaction and electron density transfer (EDT) from lone pair electrons to the antibonding orbital has been analyzed [22]. Several donor-acceptor interactions are observed for the 1,2-disubstituted benzimidazole derivatives and among the strongly occupied NBOs, the most important delocalization sites are in the π system and in the lone pairs (n) of the oxygen, fluorine and nitrogen atoms. The σ system shows some contribution to the delocalization, and the important contributions to the delocalization corresponds to the donor-acceptor interactions are C3-C4 \rightarrow C1-C2, C3-C4 \rightarrow C7-N15, C7-N15 \rightarrow C1-C2, C8-C10 \rightarrow C9-C11, C9-C11 \rightarrow C12-C13, C12-C13 \rightarrow C9-C11, C19-C28 \rightarrow C20-C22, C20-C22 \rightarrow C19-C21, LP N14 \rightarrow C2-C3 and LP N14 \rightarrow C7-N15. The charge distribution of 1,2-disubstituted benzimidazole derivatives was calculated from the atomic charges by NLO and NBO analysis (Fig. 3). These two methods predict the same trend, i.e., among the nitrogen atoms N14 and N15, N14 is considered as more basic site [23]. The charge distribution shows that the more negative charge is concentrated on N15 atom whereas the partial positive charge resides at hydrogens. When compared to nitrogen atoms (N14 and N15), fluorine atom are less electronegative in 1,2-disubstituted benzimidazole derivatives and among the nitrogen atoms N14 is considered as more basic site [24].

Molecular electrostatic potential map (MEP) and electronic properties

MEP surface diagram (Fig. S4) is used to understand the reactive behaviour of a molecule, in that negative regions can be regarded as nucleophilic centres, whereas the positive regions are potential electrophilic sites. The MEP map of benzimidazole derivatives clearly suggests that the nitrogen and fluorine atoms represent

Table 2 Electric dipole moment (μ), polarizability (α) and hyperpolarisability (β) of 1-6.

Parameter	1	2	3	4	5	6
μ_x	-0.5692	-0.0409	0.1465	-0.8743	0.1707	0.0572
μ_y	-0.0512	0.4719	-3.5160	-0.4619	-3.4644	-1.5617
μ_z	1.2996	0.5524	1.0010	0.5048	1.2082	-1.6511
μ_{tot}	0.6792	0.9834	-2.3685	-0.8314	-2.0855	3.1556
α_{xx}	287.4093	309.7633	156.3882	293.5637	-117.2774	-120.8744
α_{xy}	-1.6580	-53.0280	7.9576	28.8191	4.1861	0.6590
α_{yy}	155.8577	131.2507	-169.1891	154.5733	-137.9645	-152.7575
α_{yz}	-1.5185	28.3731	-3.2932	6.6294	-1.2303	11.5158
α_{zz}	-40.6877	-1.3015	10.4458	-11.4693	-0.4711	2.0492
$\alpha_{tot} \times 10^{-23}$	227.8743	249.4627	-162.7973	221.6728	-144.0098	-151.0374
β_{xxx}	3.3154	3.4109	-86.7455	3.3088	-1.9723	-2.0978
β_{xyy}	-608.3990	-383.9197	7.2463	-708.3375	-44.3386	111.2710
β_{yyy}	52.6782	52.4608	-69.4471	-223.2285	-39.2493	-3.5024
β_{xxy}	-35.2133	4.8141	-1.4761	-54.7116	3.5490	-25.3174
β_{yyz}	-51.1884	18.1350	15.2006	-80.5413	13.1731	10.9727
β_{xxz}	-62.6401	-47.5325	42.6434	52.4268	5.1746	-35.3616
β_{xyz}	44.8590	17.2619	0.8119	4.9552	-2.9465	-34.4533
β_{yyz}	46.2349	43.6417	-29.9926	7.5525	14.0433	-16.6196
β_{xzz}	-6.6788	-53.8138	-7.6853	-21.1557	18.7322	-13.9812
β_{yzz}	2.1320	63.1668	-16.4025	-11.6743	-18.2658	-18.5493
β_{zzz}	82.9746	-29.2103	3.6761	79.8413	-0.6432	3.9319
$\beta_{tot} \times 10^{-31}$	56.4751	39.2501	6.2666	74.0178	4.5697	7.5372
$\mu \times \beta_0 \times 10^{-31}$	38.3579	38.5985	-14.8424	61.5384	-9.5301	23.7844

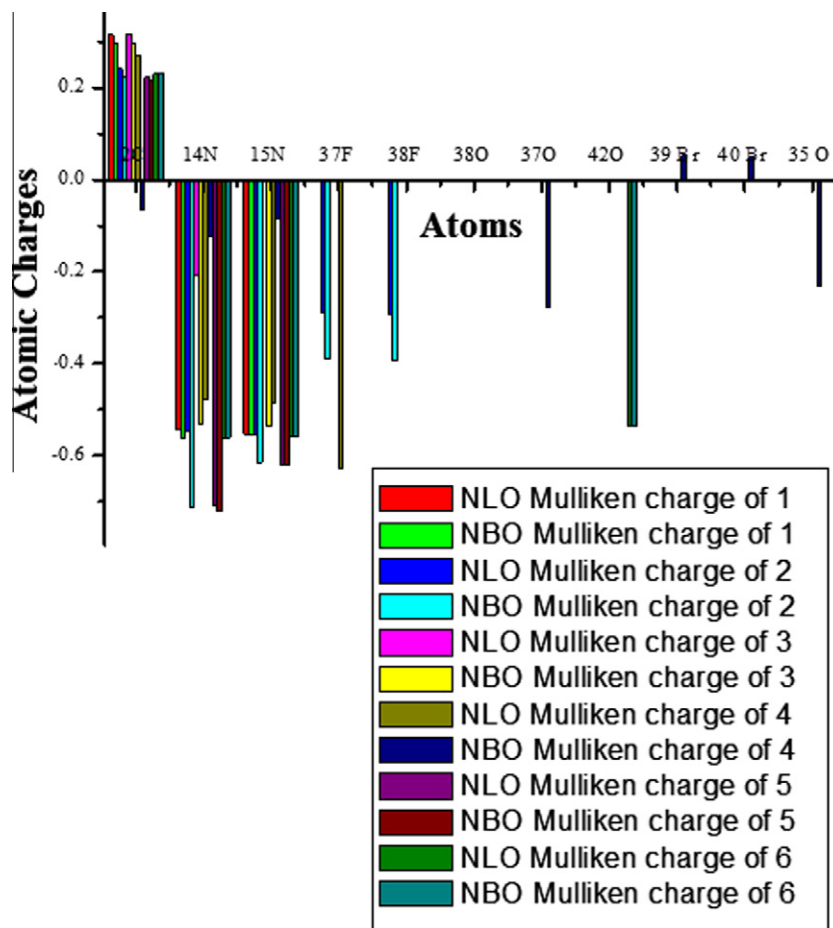


Fig. 3. Mulliken charge distribution of 1–6 using NLO and NBO methods.

the most negative potential region. The hydrogen atoms bear the maximum brunt of positive charge. The predominance of green region in the MEP surfaces corresponds to a potential halfway between the two extremes red and dark blue color.

Atoms in molecules analysis of 4

The AIM analysis was used to determine the presence of bond critical points (BCPs) of the intramolecular bonds and to evaluate their energies. The most often used criteria of the existence of hydrogen bonding interactions are the electron density $\rho(r_c)$ and the Laplacian of the electron density $\nabla^2\rho(r_c)$ at the BCPs. These parameters for the intramolecular along with the lengths and angles of the corresponding hydrogen bonds in the studied molecules are 2.012 Å, 127.8°, respectively. There is good correlation between the $\rho(r_c)$ and $\nabla^2\rho(r_c)$ values. Positive values of Laplacian $\nabla^2\rho(r_c)$ (2.001) indicative of depletion of electronic charge along the bond path, which is characteristic of closed shell interactions such as hydrogen bonds.

Conclusion

In this paper we have reported benzimidazole based chromophores as potential NLO materials. The presence of α twist in this benzimidazole drops the fluorescence quantum yield. The observed dipole moment and hyperpolarisability can be explained by the reduced planarity caused by the steric interaction in nitrogen atom attached to benzyl ring. Hence, the steric interaction must be reduced in order to obtain larger β_0 values. From the

DFT calculations, it was concluded that molecules of higher hyperpolarizability have larger dipole moments used as potential NLO molecules. The MEP map of benzimidazole derivatives clearly suggests that the nitrogen, bromine and fluorine atoms represent the most negative potential region. The hydrogen atoms bear the maximum brunt of positive charge. From AIM analysis the presence of bond critical points (BCPs) of the intramolecular bonds and their energies was evaluated.

Acknowledgments

One of the authors Prof. J. Jayabharathi is thankful to DST [No. SR/S1/IC-73/2010], UGC (F.No. 36-21/2008 (SR)) and DRDO (NRB-213/MAT/10-11) for providing funds to this research study.

Appendix A. Supplementary data

Supplementary data associated with this article can be found, in the online version, at <http://dx.doi.org/10.1016/j.saa.2012.05.085>.

References

- [1] E.M. Across, K.M. White, R.S. Moshrefzadeh, C.V. Francis, *Macromolecules* 28 (1995) 2526.
- [2] X.R. Bu, H. Li, D.V. Derveer, E.A. Mintz, *Tetrahedron Lett.* 37 (1996) 7331.
- [3] C.W. Dirk, H.E. Katz, M.L. Schilling, L.A. King, *Chem. Mater.* 2 (1990) 700.
- [4] K. Mahalingam, M. Nethaji, P.K. Das, *J. Mol. Struct.* 378 (1996) 177–188.
- [5] R. Koch, J.J. Finnerty, T. Bruhn, *J. Phys. Org. Chem.* 21 (2008) 954–962.
- [6] E. Kleinpeter, A. Koch, B. Mikhova, B.A. Stamboliyska, T.M. Kolev, *Tetrahedron Lett.* 49 (2008) 1323–1327.

- [7] C.R. Moylan, R.D. Miller, R.J. Twieg, K.M. Betterton, V.Y. Lee, T.J. Matray, C. Nguyen, *Chem. Mater.* 5 (1993) 1499.
- [8] M. Ammamm, P. Bauerle, *Org. Biomol. Chem.* 3 (2005) 4143.
- [9] S.R. Marder, J.E. Sohn, G.D. Stucky (Eds.), *Materials for non-linear optics: chemical perspectives*. In: ACS Symposium Series, vol. 455, American Chemical Society, Washington, DC, 1991.
- [10] J. Messier, F. Kajzar, P. Prasad (Eds.), *Organic Molecules for Non-linear Optics and Photonics*, Kluwer Academic, Dordrecht, 1991.
- [11] L.R. Dalton, A.W. Harper, R. Ghosn, W.H. Steir, M. Ziari, H. Fetterman, Y. Shi, R.V. Mustacich, A.K.Y. Jen, K.J. Shea, *Chem. Mater.* 7 (1995) 1060.
- [12] R.G. Benning, *J. Mater. Chem.* 5 (1995) 365.
- [13] M. Szafran, A. Komasa, E.B. Adamska, *J. Mol. Struct.* 827 (2007) 101–107.
- [14] L. Padmaja, C. Ravikumar, D. Sajan, I. Hubert Joe, V.S. Jayakumar, G.R. Pettit, O. Faurkov Neilsen, *J. Raman Spectrosc.* 40 (2009) 419–428.
- [15] C. Ravikumar, I. Hubert Joe, V.S. Jayakumar, *Chem. Phys. Lett.* 460 (2008) 552–558.
- [16] S. Rosepriya, A. Thiruvalluvar, K. Jayamoorthy, J. Jayabharathi, Antony Linden, *Acta Crystallogr. E* 67 (2011) o3519.
- [17] Y. Porter, K.M. OK, N.S.P. Bhuvanesh, P.S. Halasyamani, *Chem. Mater.* 13 (2001) 1910–1915.
- [18] M. Narayana Bhat, S.M. Dharmaprakash, *J. Cryst. Growth* 236 (2002) 376–380.
- [19] D. Steiger, C. Ahlbrandt, R. Glaser, *J. Phys. Chem. B* 102 (1998) 4257–4260.
- [20] M.J. Frisch, G.W. Trucks, H.B. Schlegel, G.E. Scuseria, M.A. Robb, J.R. Cheeseman, J.A. Montgomery, T. Vreven Jr., K.N. Kudin, J.C. Burant, J.M. Millam, S.S. Iyengar, J. Tomasi, V. Barone, B. Mennucci, M. Cossi, G. Scalmani, N. Rega, G.A. Petersson, H. Nakatsuji, M. Hada, M. Ehara, K. Toyota, R. Fukuda, J. Hasegawa, M. Ishida, T. Nakajima, Y. Honda, O. Kitao, H. Nakai, M. Klene, X. Li, J.E. Knox, P. Hratchian, J.B. Cross, C. Adamo, J. Jaramillo, R. Gomperts, R.E. Stratmann, O. Yazyev, A.J. Austin, R. Cammi, C. Pomelli, J.W. Ochterski, P.Y. Ayala, K. Morokuma, G.A. Voth, P. Salvador, J.J. Dannenberg, V.G. Zakrzewski, S. Dapprich, A.D. Daniels, M.C. Strain, O. Farkas, D.K. Malick, A.D. Rabuck, K. Raghavachari, J.B. Foresman, J.V. Ortiz, Q. Cui, A.G. Baboul, S. Clifford, J. Cioslowski, B.B. Stefanov, G. Liu, A. Liashenko, P. Piskorz, I. Komaromi, R.L. Martin, D.J. Fox, T. Keith, M.A. Al-Laham, C.Y. Peng, A. Nanayakkara, M. Challacombe, P.M.W. Gill, B. Johnson, W. Chen, M.W. Wong, C. Gonzalez, J.A. Pople, *Gaussian 03, Revision C.02*, Gaussian, Inc., Wallingford, CT, 2004.
- [21] S.F. Tayyari, S. Laleh, Z.M. Tekyeh, M.Z. Tabrizi, Y.A. Wang, H. Rahemi, *Mol. Struct.* 827 (2007) 176–187.
- [22] J. Marshal, *Ind. J. Phys.* 7213 (1988) 659–661.
- [23] P. Wang, P. Zhu, W. Wu, H. Kang, C. Ye, *Phys. Chem. Chem. Phys.* 1 (1999) 3519–3525.
- [24] G. Wang, F. Lian, Z. Xie, G. Su, L. Wang, X. Jing, F. Wang, *Synth. Met.* 131 (2002) 1–5.